

Weak localization correction to the anomalous Hall effect in polycrystalline Fe₃Im₅

P. Mitra, R. M. Misra, A. F. Hebard and K. A. M. Muttalib
 Department of Physics, University of Florida, Gainesville FL 32611

P. Wölfe
 ITKM, Universität Karlsruhe, D-76128 Karlsruhe, Germany

In situ transport measurements have been made on ultrathin (< 100 Å thick) polycrystalline Fe₃Im₅ as a function of temperature and magnetic field for a wide range of disorder strengths. For sheet resistances R_{xx} less than $3k_B$, we find a logarithmic temperature dependence of the anomalous Hall conductivity σ_{xy} which is shown for the first time to be due to a universal scale dependent weak localization correction within the skew scattering model. For higher sheet resistance, granularity becomes important and the breakdown of universal behavior becomes manifest as the prefactors of the $\ln T$ correction term to σ_{xx} and σ_{xy} decrease at different rates with increasing disorder.

PACS numbers: 73.20.Fz, 72.15.Rn, 72.10.Fk

In ferromagnetic metals the anomalous Hall (AH) effect arises, even in the absence of an applied magnetic field, as a consequence of the spin-orbit (s-o) interaction of the spin-polarized current carriers with the non-magnetic periodic lattice and/or impurities. A full understanding of the AH effect can in principle provide quantitative estimates of spin-dependent transport coefficients in magnetic materials. Current understanding is based on several proposed mechanisms: the skew-scattering model (SSM) [1], the side-jump model (SJM) [2], and more recently, a Berry phase model [3], based on an effect predicted in the 1950s [4] (for a recent review, see [5]). To calculate the AH conductivity σ_{xy}^{SSM} within the SSM one considers s-o interaction due to impurity potentials, leading to left/right handedness of the scattering cross section for electron spin $\sigma = \pm$. In general, $\sigma_{xy}^{SSM} = \sigma_{xx} - \tau_{tr}$, with σ_{xx} the longitudinal conductivity and τ_{tr} the transport relaxation time. The SJM is the consequence of a perpendicular term in the current density operator that arises from the presence of s-o coupling induced by impurity potentials.

For the thin ferromagnetic Im₅ studied here, disorder is systematically varied and quantum corrections to σ_{xy} become increasingly important. It is known that the normal Hall conductivity receives quantum corrections from weak localization (WL), $\sigma_{xy}^{WL} = \sigma_{xy} = 2 \sigma_{xx}^{WL} = \sigma_{xx}$ [6], but no Coulomb interaction corrections [7]. Within a weak scattering model the exchange contribution to the AH conductivity was found to be zero as well [8]. In experiments of Bergmann and Ye (BY) [9] on amorphous Fe₃Im₅ of a few atomic layers thickness, quantum corrections to the AH conductivity were found to be negligible. This was interpreted by the assumption of enhanced spin- \uparrow scattering, suppressing the WL contribution. Theoretically, the WL contribution to the AH conductivity, although finite in different models [8, 10], is cut off by spin- \uparrow scattering ($l = s$), by spin-orbit scattering ($l = so$), by the magnetic field inside the ferromagnet ($l = H$), and by the phase relaxation rate ($l = \nu$). Whereas $l = s$, $l = so$

and $l = H$ are T-independent, $l = \nu$ grows linearly with temperature T and leads to a logarithmic T-dependence, provided $\max(l = s; l = so; l = H) \ll l = \nu$, $l = \nu$, $l = \tau_{tr}$, which defines a temperature interval of observability of the WL contribution. Unexpectedly, $l = \nu$ in ferromagnetic Im₅ turns out to be largely due to spin-conserving inelastic scattering of spin wave excitations [11, 12], such that the above inequality is satisfied in the regime of stronger disorder and WL is experimentally observed.

We present results on two series of ultrathin Im₅ of polycrystalline iron grown at room temperature by r.f. magnetron sputtering in the Hall bar geometry through a shadow mask onto glass (type A samples) and sapphire (type B samples) substrates under slightly different deposition conditions. The experiments were performed in a specialized apparatus in which the sample can be transferred without exposure to air from the high vacuum deposition chamber to the center of a 7 T magnet located in a low temperature cryostat. Ex situ topographical scans using an AFM showed a granular morphology. To parameterize the amount of disorder in a given Im₅, we use the sheet resistance $R_0 = R_{xx}(T = 5K)$, which in the results reported here spans the range from 50 Ω (100 Å thick) to 50k Ω (< 20 Å thick). Carefully timed postdeposition ion milling of some of the Fe₃Im₅ gives rise to a decrease in resistance as large as a factor of two accompanied by a concomitant improvement of electrical homogeneity and Im₅ smoothness [13]. This postdeposition in situ treatment does not noticeably affect the dependence of our transport results on R_0 , thus indicating that R_0 rather than surface topography is a robust indicator of disorder. The AH resistivity is measured under constant current conditions in magnetic fields of 4T at selected temperatures. These fields are well above saturation where the AH signal is maximum. For each sample the longitudinal and transverse voltages are simultaneously measured so that the symmetric (R_{xx}) and antisymmetric (R_{xy}) responses can be extracted. Contribution from the normal Hall effect is negligible, as is the magnetoresistance.

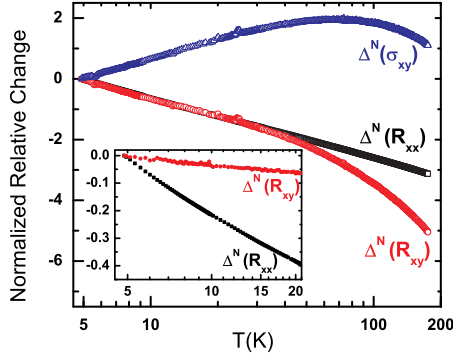


FIG. 1: $\ln(T)$ dependence of R_{xx} and R_{xy} for $T < 20K$ for a type A sample with $R_0 = 2733$. Inset: $R_0 = 49k$.

We define the "normalized relative change", $\Delta^N(Q_{ij}) = (L_0/R_0)(Q_{ij} - Q_{ij}(T_0))$ with respect to our reference temperature $T_0 = 5K < T$, where $L_0 = e^2/h$, $Q_{ij} = Q_{ij}(T) - Q_{ij}(T_0)$ and Q_{ij} refers to either resistances $R_{xx}; R_{xy}$ or conductances $\sigma_{xx}; \sigma_{xy}$. We find that for all values of $R_{xx}(T_0) = R_0$ studied, there is a range of temperatures $T < 20K$ where $\Delta^N(Q_{ij})$ has a logarithmic temperature dependence. Figure 1 shows results for a type A sample with $R_0 = 2733$. Following BY's notation [9], we define for our low temperature data

$$\Delta^N(R_{xx}) = A_R \ln \frac{T}{T_0}; \quad \Delta^N(R_{xy}) = A_{AH} \ln \frac{T}{T_0} \quad (1)$$

Using the fact that $\sigma_{xx} = 1/R_0$, and $R_{xy}(T) = R_{xx}(T)$ for our films, we have the longitudinal conductivity $\sigma_{xx} = 1/R_{xx}$ and the AH conductivity $\sigma_{xy} = R_{xy}/R_{xx}^2$, so that

$$\Delta^N(\sigma_{xx}) = A_R \ln \frac{T}{T_0}; \quad \Delta^N(\sigma_{xy}) = (2A_R - A_{AH}) \ln \frac{T}{T_0} \quad (2)$$

Figure 1 also shows that the curves for $\Delta^N(R_{xx})$ and $\Delta^N(R_{xy})$ exactly overlap each other while obeying $\ln T$ dependence up to $T = 20K$, i.e. $A_{AH} = A_R$. Fitting the low temperature data to equations (1), we find for this particular film that $A_R = 0.897 \pm 0.001$, and $A_{AH} = 0.908 \pm 0.005$. This "relative resistance" (RR) scaling, namely $A_{AH} = A_R = 1$, remains valid for type A samples in the range $500 < R_0 < 3k$ and type B samples in the more restricted range $1.5k < R_0 < 3k$, as shown in Fig. 2. In contrast, BY observed $A_R = 1$ and $A_{AH} = 2$ within the same range of R_0 and T . We note from eq (2) that $A_{AH} = A_R = 2$ implies $\Delta^N(\sigma_{xy}) = 0$. Thus while the amorphous samples of BY show no logarithmic temperature dependence of AH conductance, our polycrystalline samples show a $\ln T$ dependence with a prefactor close to unity. At lower R_0 , A_{AH} increases for both sample types with a more pronounced increase in the type B samples where $A_{AH} = A_R = 2$ and $\Delta^N(\sigma_{xy}) = 0$ at the lowest resistance $R_0 = 140$.

At higher resistances, the RR scaling for $T < 20K$ shows deviations, as seen in the inset of Fig. 1 and in Fig. 2(c). We will argue later that these deviations can be understood within a granular model. The deviations from the $\ln T$ behavior at temperatures $T > 20K$ shown in Fig. 1 seem to be non-universal, and may arise from phonon scattering. This high temperature region could not be studied by BY because their quenched condensed films irreversibly annealed. We will restrict our theoretical analysis to the low temperature regime only.

We describe the ferromagnetic film as a quasi-two-dimensional system of conduction electrons with Fermi energies ϵ_F depending on the spin index $\sigma = \uparrow, \downarrow$, and with spin-orbit coupling g . The Coulomb interaction will be considered later as a perturbation. We model the total impurity potential as a sum over identical single impurity potentials $V(\mathbf{r} - \mathbf{R}_j)$ at random positions \mathbf{R}_j . The Hamiltonian is given by

$$H = \sum_{\mathbf{k}} (\epsilon_{\mathbf{k}} - \epsilon_F) c_{\mathbf{k}\sigma}^\dagger c_{\mathbf{k}\sigma} + \sum_{\mathbf{k}, \mathbf{k}'; 0 \leq j} V(\mathbf{k} - \mathbf{k}') e^{i(\mathbf{k} - \mathbf{k}') \cdot \mathbf{R}_j} f_{0j}^\dagger g c_{\mathbf{k}'0}^\dagger c_{\mathbf{k}0} \quad (3)$$

where σ is a Pauli matrix, and $\mathbf{k}; \mathbf{k}'$ are unit wave vectors. For simplicity we assume isotropic band structure and expand the dependence on scattering angle in angular momentum eigenfunctions e^{im} , keeping only the s-wave component V of the impurity potential. In terms of the real and imaginary parts of the $m = 1$ eigenvalue of the particle-hole ladder $\chi_1 = \chi_1^0 + i\chi_1^1$, we find the spin independent parameters $\chi_{tr} = (1 \quad 0)$ and $\chi^- = \chi_1^0 - g \tau N_0 V$ where N_0 is the average DOS

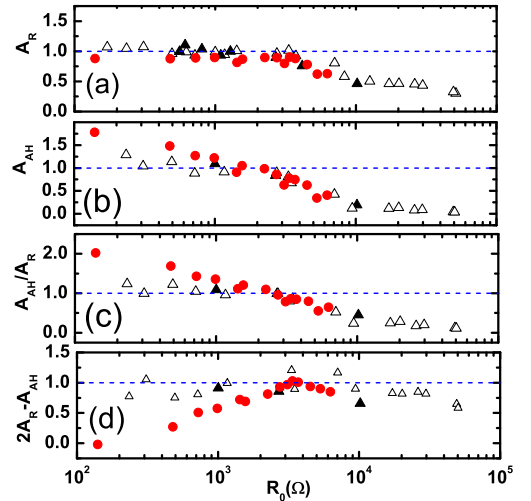


FIG. 2: Coefficients A_R and A_{AH} as defined in Eq. 1 for type A (triangles) and type B (circles) samples. Solid triangles represent type A samples that have undergone surface modification and conductance changes associated with post-deposition ion milling as described in text.

at the Fermi level and τ is the single particle relaxation time. Keeping only the main dependencies on spin, that of k_F , the longitudinal and the AH conductivities of this model are given in the weak scattering limit by

$$\frac{R_{xy}^{SSM}}{R_{xx}^{SSM}} = \frac{0}{1} - M g_{so} \tau = ; \quad \frac{R_{xy}^{SJM}}{R_{xx}^{SJM}} = e^2 M g_{so} \tau = ; \quad (4)$$

where $\frac{0}{xx} = e^2 (n \tau) / \tau$, $g_{so} = g = 4 n$ and $M = n \tau$ is the net spin density. While these equations are consistent with conventional results $R_{xy}^{SSM} / R_{xx}^{SSM}$ and $R_{xy}^{SJM} / R_{xx}^{SJM}$, being the resistivity, we note that the ratio $\frac{R_{xy}^{SJM}}{R_{xy}^{SSM}} = \frac{SJM}{SSM}$ can in fact decrease with increasing R_0 , as we demonstrate later, if τ increases sufficiently rapidly with disorder, especially since disorder in our thin films is characterized by the sheet resistance R_0 rather than the resistivity.

Turning now to the quantum corrections, we first calculate [14] that there is no interaction induced ln T correction to R_{xy} . This holds for both exchange and Hartree terms, for both the skew scattering and the side-jump models. It generalizes the result reported in [8]. To see if WL corrections are important, we need an estimate of the phase relaxation rate τ^{-1} . While the contribution from e-e-interaction $\tau^{-1} = (\Gamma = \Gamma_{tr}) \ln(\Gamma_{tr} = 2)$ is small, a much larger contribution is obtained from scattering of spin waves [11, 12], $\tau^{-1} = 4 (J^2 = \Gamma_g) T$, where $J \approx 160K$ is the exchange energy of the s-electrons and $\Gamma_g = (k_B) (m \tau) B_{in}$ is the spin-wave gap, where the internal field B_{in} is in Tesla and m is the effective mass. For thin films with $150 < R_0 < 3k$ we find $\Gamma_{tr} < 10$. Thus the WL condition $\tau \tau^{-1} < 1$, with $\tau \tau^{-1} = 4 (\Gamma_{tr}) (eB_{in} = m c)$, can be satisfied down to 5K observing that $B_{in} = B_{ex}$ for a thin slab and taking $m = m = 4$ [15]. The s-o relaxation rate $\tau_{so}^{-1} = \tau_{tr}^{-1} g^2 = \tau_{tr}^{-1} 10^3 = \tau_{tr}^{-1} 0.5 \cdot 10K$ (using $g_{xy} = g_{xx}$), which is at the border or below the considered temperature regime. We have no indication of spin- \uparrow scattering in our samples. Also, τ is seen to be much larger than τ_{tr} for all temperatures considered. We are therefore confident that WL has been seen in our data.

Calculating the diagrams shown in Fig. 3, we find

$$\frac{W_{xx}^L}{R_{xx}^L} = L_0 \ln(\tau =); \quad \frac{W_{xy}^L}{R_{xy}^L} = \frac{W_{xx}^L}{R_{xx}^L} - M g_{so} \tau = ; \quad (5)$$

The WL contribution from the side-jump model is zero in the approximation where only the dependence of k_F is kept and is generally small [10]. Using $\tau = 1/T$, it follows from Eqs. (4) and (5) that the normalized WL correction to the Hall conductivity is given as

$$\frac{N_{xx}^{WL}}{R_{xx}^L} = \ln \frac{T}{T_0}; \quad \frac{N_{xy}^{WL}}{R_{xy}^L} = \frac{R_{xy}^{SSM} \ln(\Gamma = T_0)}{(R_{xy}^{SSM} + R_{xy}^{SJM})}; \quad (6)$$

where $\frac{0}{xx} = 1 = R_0$. Comparing with Eq. (2), this corresponds to $A_R = 1$ and $2A_R = A_{AH} = [R_{xy}^{SSM} = (R_{xy}^{SSM} + R_{xy}^{SJM})]$. Assuming that $\frac{R_{xy}^{SJM}}{R_{xy}^{SSM}} = \frac{SJM}{SSM}$ is a function of R_0 decreasing from values ≈ 1 at $R_0 \approx 150$ to values

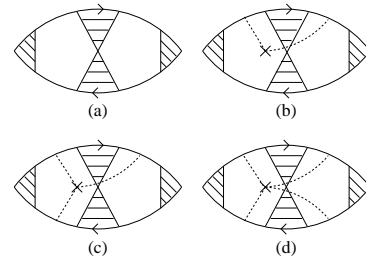


FIG. 3: Weak localization diagrams. Solid lines are impurity averaged Green's functions, broken lines are impurity scattering amplitudes [5, 14]), shaded cross is the Cooperon $C(Q; i!_1) = (2 N_0 \tau^2)^{-1} [j!_1 j + D^p Q^2 + \dots]^{-1}$ where D^p is the diffusion constant in the particle-particle channel [16], and the triangles are current vertex corrections. There are two diagrams of type (b) and four diagrams of type (c)

1 at $R_0 \approx 3k$, as discussed earlier, we find good agreement with our experimental data, if $\frac{R_{xy}^{SJM}}{R_{xy}^{SSM}} = \frac{SJM}{SSM}$ is small in samples of type A, and large in samples of type B at weak disorder. The above interpretation can also account for the BY data on amorphous films, provided that $\frac{R_{xy}^{SJM}}{R_{xy}^{SSM}} = \frac{SJM}{SSM}$ is assumed to be sufficiently large [17] and the interaction contribution to R_{xx} is small due to a cancellation of exchange and Hartree terms [8]. One then obtains $N_{xx} = \ln(\Gamma = T_0)$ and $N_{xy} = 0$ corresponding to $A_R = 1$ and $A_{AH} = 2$ as seen in the BY experiment. It is also consistent with data on Fe/Si multilayers [19] where the ratio $A_{AH} = A_R$ was found to be intermediate between BY and RR scaling.

We now turn to the regime $R_0 > 3k$, where both A_R and A_{AH} systematically decrease as R_0 increases, but at different rates, as shown in Fig. 2. For example, for a type A sample with $R_0 = 49k$, $A_R = 0.326$ and $A_{AH} = 0.042$, so that the ratio $A_{AH} = A_R \approx 1$. We will now argue that a granular model for our polycrystalline films explains many of the qualitative features. As the grains become more weakly coupled the AH resistivity is dominated by intragranular (rather than intergranular) skew scattering processes suffered by an electron when it is multiply reflected off the grain boundary back into the grain. We may therefore identify $R_{xy} = R_{xy}^g$, where R_{xy}^g is the Hall resistivity of a single grain. Accordingly, in the low resistance regime the longitudinal resistivity $R_{xx} = R_{xx}^g + R_{xx}^T$ is dominated by R_{xx}^g arising from the scattering at the grain boundaries while in the high resistance regime the tunneling process dominates so that $R_{xx} \approx R_{xx}^T$. Since R_{xy}^g is independent of R_{xx}^T in this regime, the quantity $R_{xy} = R_{xy} = R_{xy}^g = R_{xy}^g$ should be independent of R_0 as is indeed the case as shown in Fig. 4 for type A films with three different R_0 .

Additional support for the granular model is found by inverting the resistivity tensor to find $\frac{R_{xy}}{R_{xx}} = \frac{R_{xy}^g}{R_{xx}^T} = (R_{xx}^T)^{-2}$. It then follows that $\frac{R_{xy}}{R_{xx}} = \frac{R_{xy}^g}{R_{xx}^T} = 2 \frac{T}{R_{xx}^T} = \frac{T}{R_{xx}^T} + (\frac{g_{xy}}{R_{xx}^T} = \frac{g_{xy}}{R_{xx}^T})$. Since our previous calculations remain valid

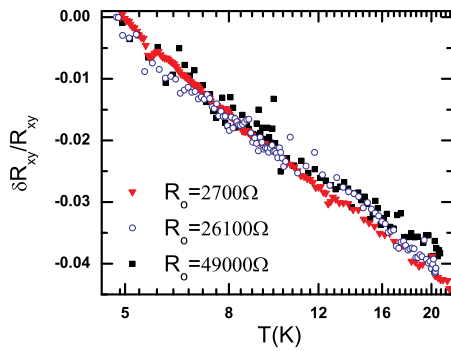


FIG. 4: $\ln(T)$ dependence of relative changes in the AH resistance for type A films with three different R_0 .

within a single grain, we can use our calculated values $A_R^g = 1$ and $A_{AH}^g = 1$ for the two terms in parentheses. Using $\frac{R_{xx}^T}{R_{xx}^0} = \frac{R_{xx}^T}{R_{xx}^0} = A_R R_0^T L_{00} \ln(T=T_0)$, this yields the relation $\ln\left(\frac{R_{xx}^T}{R_{xx}^0}\right) = (2A_R R_0^g = R_0^T) \ln(T=T_0)$. Comparing with eq. (2) we obtain $A_{AH} = R_0^g = R_0^T$. Since the grain properties are independent of R_{xx}^T , it follows that $A_{AH} = 1/R_0^T$. Figure 2 shows that this is indeed the case, where $A_{AH} \neq 0$ and the combination $2A_R A_{AH} = 2A_R$ for large R_0 . Although we can not evaluate A_R separately to explain why $A_R \neq 0.5$ in this regime, we do expect A_{AH} to be smaller than A_R , as seen in the inset of Fig. 1 and in Fig. 2, since A_R involves only tunnelling resistances while A_{AH} involves a ratio of $R_0^g = R_0^T = 1$. Note, however, that there is an additional $\ln T$ contribution of the interaction type due to the scattering of electrons by the ferromagnetic spin waves: $\frac{W^L}{s L_{00} (F_{tr})^2} (J_F) \ln(\nu, \omega)$, which has the opposite sign, and increases with the disorder strength [14]. This might possibly lead to a drop of A_R beyond $3k$.

We note that within a granular model, the weak localization contribution to ρ_{xx} and the exchange part of the interaction contribution have been shown to lead to $A_R^{WL} = 1$ and $A_R^{ex} = 1$, respectively [20]. However, the Hartree contribution to A_R has not yet been calculated for such a model. We expect that it will tend to cancel the exchange contribution just as in the weakly disordered samples [18]. The "high temperature" $\ln T$ correction to the longitudinal resistivity found in [21] would appear at temperatures $T \gg \epsilon$, above the range studied here. We estimate the inverse escape time $\tau = g\epsilon$, where g is the dimensionless conductance and ϵ is the average energy level spacing within a 1 nm granule as $\epsilon \approx 50K$.

In conclusion, we have investigated the charge transport properties of ultrathin films of iron grown in-situ under well-controlled conditions, excluding in particular unwanted oxidation or contamination. Polarizing the magnetic domains by an applied magnetic field induces a strong anomalous Hall effect signal. We observe logarithmic temperature dependencies in both the Hall and the longitudinal conductance over a wide range of tempera-

ture and sheet resistance, which is a hallmark of quantum corrections in 2D. For sheet resistance $R_0 < 3k$ in type A samples on glass substrates the logarithmic corrections obey a heretofore unobserved 'RR scaling' that is found to be nearly independent of R_0 which is interpreted in terms of weak localization corrections within the skew scattering model. In the same regime the type B samples grown on sapphire substrates show with increasing disorder a continuous increase of the normalized coefficient of the $\ln T$ term in ρ_{xy} , which we interpret as a weak localization correction in the presence of a sizeable but decreasing side-jump contribution. This interpretation may be extended to the higher resistance samples, for which the logarithmic corrections are found to decrease with increasing R_0 , if the granular nature of these samples is taken into account. Accordingly, it appears that tunneling resistances between the grains dominate the longitudinal transport, while the Hall transport is still controlled by scattering processes within a single grain. Thus the observed R_0 dependence of the anomalous Hall effect and its quantum corrections may be explained by assuming skew scattering as well as the side-jump mechanism to be operative in our samples. Quantum corrections of the interaction type turn out to play a minor role, with the possible exception of an anti-localizing contribution due to scattering of spin waves in the high resistance regime.

We thank I. Gomyi, D. Maslov and A. D. Mirlin for useful discussions. This work has been supported by the NSF under Grant No. 0404962 (AFH), a Max-Planck Research Award (PW, KAM) and by the DFG-Center for Functional Nanostructures (PW).

Corresponding author: afh@phys.u.edu

- [1] J. Smit, Physica (Amsterdam) 21, 877 (1955); Phys. Rev. B 8, 2349 (1973).
- [2] L. Berger, Phys. Rev. B 2, 4559 (1970).
- [3] G. Sundaram and Q. Niu, Phys. Rev. B 59, 14915 (1999).
- [4] R. Karplus and J.M. Luttinger, Phys. Rev. 95, 1154 (1954).
- [5] P. Woelke and K.A. Muttalib, Ann. Phys. (Leipzig) 15, 508 (2006).
- [6] H. Fukuyama, J. Phys. Soc. Jpn. 49, 644 (1980).
- [7] B.L. Altshuler, D. Khmel'nitskii, A.I. Larkin, and P.A. Lee, Phys. Rev. B 22, 5142 (1980).
- [8] A. Langenfeld and P. Woelke, Phys. Rev. Lett. 67, 739 (1991).
- [9] G. Bergmann and F. Ye, Phys. Rev. Lett. 67, 735 (1991).
- [10] V.K. Dugaev, A. Crepieux, and P. Bruno, Phys. Rev. B 64, 104411 (2001).
- [11] G. Tatara, H. Kohno, E. Bonet, and B. Barbara, Phys. Rev. B 69, 054420 (2004).
- [12] M. Plihal, D.J. Mills and J. Kirshner, Phys. Rev. Lett. 82, 2579 (1999).
- [13] P. Mitra and A.F. Hebard, Appl. Phys. Lett. 86, 063108 (2005).

- [14] K. A. Muttalib and P. W. Lee, to be published.
- [15] R. Q. Hood, and L. M. Falicov, Phys. Rev. B 46, 8287 (1992).
- [16] D^p is equal to the usual diffusion coefficient $D = \frac{1}{2} v_F^2 \tau$ up to terms of order g^2 .
- [17] In amorphous Fe films the side jump mechanism has been shown to dominate, see G. Bergmann and M. Zhang, eprint cond-mat/0501321, as proposed in [10]
- [18] The interaction correction may be small due to strong screening, causing the exchange and Hartree terms in the interaction correction result $\chi_{xx} = L_{00} (1 - \frac{3}{4} \tilde{F}) \ln(T)$ to cancel (for bulk Fe one estimates $\tilde{F} \approx 1$).
- [19] Y. K. Lin et al, Phys. Rev. B 53, 4796 (1996)
- [20] I.S. Beloborodov, A.V. Lopatin, and V.M. Vinokur, Phys. Rev. Lett. 92, 207002 (2004); I.S. Beloborodov et al, Phys. Rev. Lett. 91, 246801 (2003).
- [21] K.B. Efetov, and A. Tschersich, Europhys. Lett. 59, 114 (2002).